

Control of muscle regeneration in the *Xenopus* tadpole tail by Pax7

Ying Chen, Gufa Lin and Jonathan M. W. Slack*

The tail of the *Xenopus* tadpole will regenerate completely after transection. Much of the mass of the regenerate is composed of skeletal muscle, but there has been some uncertainty about the source of the new myofibres. Here, we show that the growing tail contains many muscle satellite cells. They are active in DNA replication, whereas the myonuclei are not. As in mammals, the satellite cells express *pax7*. We show that a domain-swapped construct, *pax7EnR*, can antagonize *pax7* function. Transgenic tadpoles were prepared containing *pax7EnR* driven by a heat-inducible promoter. When induced, this reduces the proportion of satellite cells formed in the regenerate. A second amputation of the resulting tails yielded second regenerates containing notochord and spinal cord but little or no muscle. This shows that inhibition of *pax7* action does not prevent differentiation of satellite cells to myofibres, but it does prevent their maintenance as a stem cell population.

KEY WORDS: Pax7, Pax7EnR, Muscle satellite cells, Regeneration, *Xenopus laevis*

INTRODUCTION

Following amputation, the tail of the *Xenopus* tadpole will regenerate over 2-3 weeks to restore a functional appendage of similar size to the original (Slack et al., 2004). Much of the tissue mass of the regenerated tail consists of striated muscle, but the origin of this muscle has been a matter of some uncertainty and controversy. In this paper, we show that an adult stem cell: the muscle satellite cell, already known to be able to replace fibres in damaged muscle, is also capable of building a new mass of tissue in an extended regenerated appendage.

In principle, three possibilities have been proposed for the origin of regenerated muscle: de-differentiation of myofibres, muscle satellite cells and side population (SP) cells. During regeneration of the limbs of urodele amphibians (newts and salamanders), it has been well documented that the striated muscle fibres can de-differentiate (Namenwirth, 1974; Lo et al., 1993; Kumar et al., 2000; Echeverri et al., 2001). In this process, the nuclei of the myofibres re-enter S-phase and the fibres break apart to become mononuclear cells. These cells then participate in the regeneration blastema, proliferate and eventually become re-differentiated, mostly as new myofibres, but also as some other tissue types. In postnatal mammals, there is no regeneration of appendages such as limbs or tails. However, striated muscle does have some ability to repair itself following tissue damage. In this process, the new fibres are generally considered to be derived from muscle satellite cells: a population of small mononuclear cells located beneath the basement membrane of the myofibres (Seale and Rudnicki, 2000). Muscle satellite cells can be considered as a type of adult stem cell as they are able both to reproduce themselves and to produce myoblasts, which can differentiate to form new myofibres. However, this idea has been challenged because in skeletal muscle, there also exists another kind of stem cell called side population (SP) cells that can be recognized by a DNA-binding Hoechst (33342) dye (Gussoni et

al., 1999; Jackson et al., 1999; Seale et al., 2001). Transplanted SP cells have also been shown to be able to adopt the myogenic lineage and to participate in muscle repair.

Previous studies of *Xenopus* tail regeneration showed that there was no de-differentiation of the myofibres (Ryffel et al., 2003; Gargioli and Slack, 2004). The fibres near the cut surface simply degenerate and die. This suggested a different mode of muscle regeneration from that found in urodeles. It was conjectured, on the basis of the labelling patterns from different types of graft, that satellite cells might be the precursors of the striated muscle of the regenerate (Gargioli and Slack, 2004). In the present paper, we show that this is the case. We show that, as in mammals, Pax7 is expressed in muscle satellite cells and that many satellite cells, but not myonuclei, are active in DNA replication. We show that a domain swap inhibitor, Pax7EnR, can antagonise the biological activity of Pax7. We then use an inducible *pax7EnR* transgene to deplete the tail of satellite cells and show that this reduces or inhibits the regeneration of new muscle.

Muscle satellite cells were actually first discovered in frogs, visualised by electron microscopy as mononucleated cells wedged between the basement membrane and the plasma membrane (Mauro, 1961). Later, muscle satellite cells were also found in skeletal muscles of mammals and birds, and their role in muscle repair has been studied recently (Chargé and Rudnicki, 2004). Upon muscle injury, quiescent satellite cells residing in the damaged myofibres are rapidly activated to re-enter the cell cycle. The upregulation of Myf5 and MyoD, two myogenic regulatory factors, confers on them a myoblast identity. After proliferation, most of the cells differentiate and fuse to generate new myofibres (Cornelison and Wold, 1997; Cooper et al., 1999). A minority of satellite cells are retained in the sub-laminar location to replenish the pool of cells for subsequent muscle repair (Chargé and Rudnicki, 2004).

An important gene expressed in satellite cells is *pax7* (Seale et al., 2000; Halevy et al., 2004). It is a member of the Pax (paired box) family of transcription factors, which play important roles in cell fate, early embryonic patterning and organogenesis (Mansouri et al., 1996; Mansouri et al., 1999; Ziman et al., 2001a; Lamey et al., 2004). Pax7 has three conserved protein domains, a DNA-binding domain called the paired domain, a paired-type homeodomain and an octapeptide (Jostes et al., 1990). Early studies of the *pax7* gene

Centre for Regenerative Medicine, Department of Biology and Biochemistry, University of Bath, Bath BA2 7AY, UK.

*Author for correspondence (e-mail: j.m.w.slack@bath.ac.uk)

mainly focused on its biological function in the central nervous system because of its abundant expression there (Mansouri et al., 1996; Kawakami et al., 1997; Ziman et al., 2001a). Its activity in muscle satellite cells has been established more recently (Seale et al., 2000). It has been found that Pax7 is only expressed in quiescent and newly activated muscle satellite cells. Upon myogenic differentiation, it is rapidly downregulated. The *Pax7*^{-/-} mice contain reduced number of muscle satellite cells and they are progressively lost during postnatal growth (Oustanina et al., 2004; Kuang et al., 2006; Relaix et al., 2006). These findings revealed an important feature of satellite cells in their capacity for self renewal and the role of Pax7 in this context (Zammit et al., 2004; Collins et al., 2005; Montarras et al., 2005).

Our results presented here show that the satellite cells are dividing during normal tail growth and, most importantly, that they are responsible for forming the muscle masses of the regenerated tail. This means that the cellular processes of regeneration in the anuran tadpole is much more akin to the tissue repair events of mammals than to the de-differentiation/re-differentiation process found in urodeles.

MATERIALS AND METHODS

Embryos and tadpoles

Xenopus laevis embryos were obtained by in vitro fertilization and staged according to the Nieuwkoop and Faber (NF) tables (Nieuwkoop and Faber, 1967). Embryos were dejellied with 2% cysteine (Sigma) (pH 7.8) and then cultured in 0.1×NAM. From stage 46, they were transferred to recirculating aquarium and fed on tadpole diet (Blades Biological, Redbridge, UK).

Plasmid construction

Xenopus pax7 (*Xpax7*) gene was isolated from cDNA of stage 25 embryos by RT-PCR. The primers were designed according to the sequence submitted by the laboratory of Dr Richard Harland (NCBI:AF725267): sense primer, 5'-CAA CTT GTG AGC ACT CTT CTA GGC T-3'; antisense primer, 5'-TTT TCA CCA AGT GGC AGA CAT-3'. The *pax7* DNA fragment obtained by RT-PCR was ligated into *pGEM-T easy* vector (Promega) to generate *pax7-pGEMT*, which was then sequenced. The full-length *Xenopus pax7* gene was excised from *pax7-pGEMT* plasmid by *SpeI* and *ApaI* (Promega), and cloned into *SpeI* and *ApaI* sites of *pSL1180* vector (Amersham). This plasmid is called *pax7-pSL1180* and used for subsequent cloning.

To generate the construct for RNA injection, the full *pax7* sequence was isolated from *pax7-pSL1180* with *HindIII* and *EcoRI* (Promega) and cloned into the same sites of *pcDNA3* vector (Invitrogen). Capped *Pax7* RNA was then transcribed in vitro with *T7* RNA polymerase (Promega) after linearization with *Tth1111* (Promega).

The dominant-negative form of *pax7* was made by the following steps. The N-terminal region of the *Xenopus pax7* gene (1-245 amino acids) was excised from *pax7-pSL1180* with *HindIII* and *SmaI* (Promega), and was then cloned into *HindIII* and *Clal* (blunt filled) sites of *ENR-N-pCS2+* vector (kind gift of Dan Kessler). This *pax7EnR* plasmid is designed to produce a fusion protein, which includes the *pax7* DNA-binding domain and *Drosophila engrailed* repressor domain. For RNA injection, the sequence of *pax7EnR* was cloned into *pcDNA3* with *HindIII* and *XbaI* (Promega) to generate *pax7EnR-pcDNA3*. This plasmid was then linearized with *SmaI* and transcribed in vitro with *T7* RNA polymerase.

A *pax7EnR* plasmid suitable for transgenesis was made by excising the sequence of *pax7EnR* from *pax7EnR-pcDNA3* with *HindIII* and *XbaI* (blunt filled), and then cloning into *HindIII* and *SmaI* sites of *HGEM*. The *pax7EnR-HGEM* was linearized with *XmnI* before use in transgenesis.

Transgenic *Xenopus* tadpoles

Transgenic *Xenopus laevis* tadpoles were made as previously described (Amaya and Kroll, 1999), except for the omission of restriction enzyme from the reaction. The transgenics were sorted out by GFP expression in the lens at stage 42.

Microinjection

For *Pax7* overexpression, 500 pg *pax7* and 80 pg *gfp* mRNA were injected into one side of dorsal animal hemisphere at the four-cell stage. For *pax7EnR* injection, 200 pg *pax7EnR*, together with 80 pg *gfp* mRNA, was injected into one side of dorsal animal hemisphere at the four-cell stage. For rescue experiments, 500 pg *pax7*, 200 pg *pax7EnR* and 80 pg *gfp* mRNA were co-injected.

BrdU injection

The tadpoles at stage 49 were anaesthetized in 0.02% MS222, and injected with 2 μl of the thymidine analog 5-bromo-2'-deoxyuridine (BrdU) labelling reagent from the Cell Proliferation Kit (Amersham). The injection was performed 24 hours before fixation.

In situ hybridization and immunohistochemistry

Whole-mount in situ hybridization was performed according to the standard protocol (Harland, 1991). The antisense *pax7* probe was designed to hybridize specifically with the C-terminal region of *Pax7*. The *pax7-pGEMT* was linearized with *SmaI* and transcribed with *T7* RNA polymerase. For morphology or immunohistochemistry, embryos or tadpoles were fixed in Zamboni's fixative (40 mM NaH₂PO₄, 120 mM Na₂HPO₄, 2% PFA, 0.1% saturated picric acid) overnight at 4°C. Myofibres were stained with 12/101 monoclonal antibody (Kintner and Brockes, 1984) at 1:100 dilution of medium. The secondary antibody was horse anti-mouse IgG whole molecular alkaline phosphatase-conjugated (Vector Labs) at 1:1000 dilution. The colour was developed with the BM purple reagent (Roche).

Activated satellite cells were stained with MyoD monoclonal antibody (kind gift of John Gurdon) at 1:4 dilution. The basement membrane of myofibres was stained with laminin (Sigma) at 1:100 dilution. Their secondary antibodies were Texas Red-conjugated anti-mouse IgG and fluorescein-conjugated anti-rabbit IgG (Vector Labs), respectively. The monoclonal PCNA antibody (Dako Cytomation) was used at 1:500 dilution. Muscle satellite cells were stained with anti-Pax7 monoclonal antibody (Developmental Studies Hybridoma Bank, University of Iowa) at 1:300 dilution. Antigen retrieval was performed for Pax7 antibody staining by boiling the slides in citrate buffer (Vector Labs) for 5 minutes in the microwave oven. For vibratome sections, the secondary antibody was horse biotinylated anti-mouse IgG (Vector Labs) at 1:500 dilution. Then the sections were incubated in ABC reagent (Dako Cytomation), followed by colour development using a DAB kit (Vector Labs). For paraffin sections, Pax7 antibody staining was either used with the ABC method as described above, or with a fluorescence method. In the latter case, the secondary antibody is Texas Red-conjugated anti-mouse IgG (Vector Labs). The slides were counterstained in 0.5% Methyl Green solution (Fluka) and mounted in Depex (BDH) or Gel mounting medium (Biomed) before observation under the microscope.

Electron microscopy

The tadpoles at stage 49 were fixed in Zamboni's fixative containing 0.5% glutaraldehyde overnight at 4°C, washed in PBS and embedded in 5% low melting agarose (Sigma). Transverse sections (100 μm) were cut with a Leica vibratome and then immunostained as described above. Following this, the vibratome sections were washed in PBS, and post-fixed in osmium tetroxide (1% w/v) in 0.1 M sodium cacodylate buffer (pH 7.6) for 1 hour. The post-fixed sections were dehydrated in a series of ethanol and embedded in Epon resin (TAAB). The polymerized resin blocks were trimmed and transversely sectioned with a Reichert Ultracut-E ultramicrotome (Leica, Wein, Austria). Sections (100 nm) were collected onto copper grids, some being stained with uranyl acetate and lead citrate, and examined under a JEOL JEM1200EX transmission electron microscope (JEOL, Tokyo, Japan). Owing to the narrow spacing between each section, for the morphometric studies a nucleus within myofibers was counted only once in each resin block.

Tail amputation, heat shock and satellite cell counting

The *Xenopus laevis* tadpoles were anaesthetized in 1/3000 MS222 and kept in the anaesthetic solution during the operation. For the heat-shock experiments, tadpoles were placed into warmed water at 34°C for 30 minutes 3 hours before tail amputation and again each day during tail regeneration.

Initially, the distal 50% length of the tail was removed. Twelve or 14 days later, when the tail regenerated to its full length, the distal 75% of the regenerated tail was amputated again. The tadpoles were allowed to recover from anaesthesia in tap water before returning to aquarium tanks.

Muscle satellite cell counting was based on the Pax7 antibody labelling on tissue cross-sections of regenerated tails. Cells were counted on a series of sections comprising the 50 μ m length of the tail that is nearest to the first amputation site or near to the second tail amputation site, as the regenerated muscle near the tail tip is too small for any quantification. Ten tails of similar size in each group were examined and statistical analysis was performed using Student's *t*-test.

RT-PCR

Ten regenerating tails of each experimental group were collected for RNA isolation. Total RNA was prepared using Trizol and reverse transcribed into cDNA with Superscript III system (Invitrogen). Primers used for *pax7EnR* are: sense, 5'-GCTCTGTCCCCTCAGGTTTAGT-3'; antisense, 5'-GGTGGTGTGCGTCTGATTGTG-3'. Primers for *pax7* are: sense, 5'-TCA-ATAATGGTCTCTCCCCGC-3'; antisense, 5'-TTGCCAGGTAATCAA-CAGCGG-3'. Primers for *pax6* are: sense, 5'-GCA ACC TGG CGA GCG ATA AGC-3'; antisense, 5'-CCT GCC GTC TCT GGT TCC GTA GTT-3'.

TUNEL assay

For apoptosis detection, paraffin tissue sections were prepared as described above. The TUNEL assay was applied on 7 μ m section with the in situ cell death detection kit (Roche) as instructed, followed by colour development with Fast Red (tablets from Sigma). For detection of apoptosis in Pax7-expressing cells, Pax7 immunohistochemistry was carried out first, developed with DAB, and then the apoptosis labelling reaction performed and visualized with a GFP filter set. For detection of apoptosis in MyoD-expressing cells, MyoD immunohistochemistry was performed first, and then followed by the apoptosis labelling reaction. Apoptotic cells were counted in three series of sagittal sections of 3 days regenerated tails.

Photography and microscopy

GFP was observed in live tadpoles under anaesthesia as described above, using a Leica Fluo III fluorescent dissecting microscope with a GFP2 filter set. Stained sections were visualized with a Leica DMRB microscope. Images were captured using a SPOT RT camera (Diagnostic instruments) and processed with Photoshop software (Adobe).

RESULTS

Expression of *pax7/Pax7* in *Xenopus laevis*

We isolated the *Xenopus pax7* (*Xpax7*) gene from cDNA of stage 25 *Xenopus laevis* embryos by RT-PCR according to the sequence submitted by Harland's laboratory (NCBI: AY 725267). The expression pattern was determined by in situ hybridization with a *pax7*-specific antisense probe. *Pax7* transcripts are first detectable at stage 13 as two bilateral stripes in the neural plate (Fig. 1A). At stage 16, *pax7* is expressed with the highest intensity in the anterior neural fold (Fig. 1B). Transverse section of the anterior region shows that the expression domain is in the sensorial layer of the neural ectoderm and the dorsal lateral somitic mesoderm (inset in Fig. 1B). As the neural folds fuse, *Pax7* transcripts become restricted to the future brain (Fig. 1C). At tailbud stage, *pax7* expression in the head extends from the forebrain to the hindbrain and, by stage 35, to the whole spinal cord. The transcripts in the spinal cord are all concentrated on the dorsal side (Fig. 1G,J,L). From the early tailbud stage, two semi-circles of *pax7* expression in head mesenchyme cells are evident surrounding the eye (Fig. 1D-F). Cross and horizontal sections show that it is expressed in the mesenchyme cells in the dorsal and anterior region of the developing eye (Fig. 1H,M,N). Moreover, *pax7* transcripts are also detected in the pituitary anlage (Fig. 1F, inset; Fig. 1I) and in the pronephric anlage (Fig. 1E,J). A horizontal section through the pronephric anlage showed two strips of *pax7* transcripts are present in the posterior region (Fig. 1J,K).

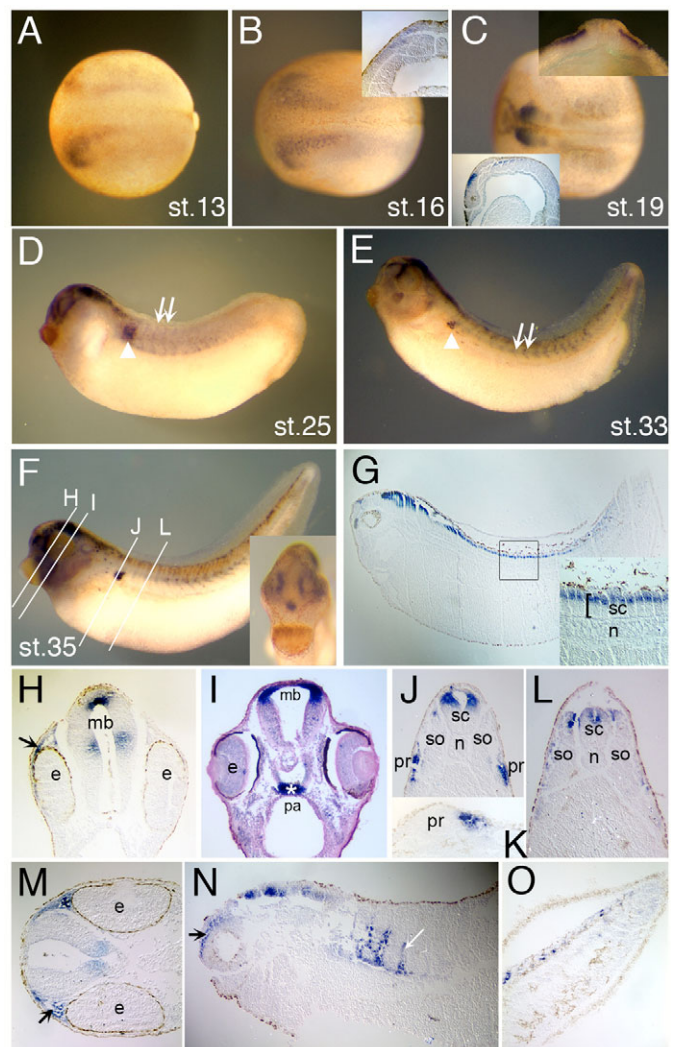


Fig. 1. Expression pattern of *pax7* in *Xenopus* early development.

Whole-mount in situ hybridization was performed with the *pax7* antisense RNA probe. (A-C) Dorsal view of stage 13 (A), stage 16 (B) and stage 19 (C) embryos, anterior towards left. The inset in B is an anterior transverse section of a stage 16 embryo, showing that *pax7* is expressed in the sensorial layer of neural ectoderm and in the lateral plate mesoderm. The inset in the bottom left-hand corner in C shows the segmented pattern of *pax7* expression in a stage 19 embryo. The inset in the top right-hand corner is a view of an anterior transverse section. (D-F) Lateral view of stage 25, 33 and 35 embryos, anterior towards left. The arrowheads in D,E indicate the expression domain of *pax7* in the pronephros. Arrows in D,E show the chevron pattern of *pax7* expression in somites. The inset in F is an anterior view of stage 35 embryo. The lines in F indicate the relative position of cross-section planes in H-J,L. (G) Sagittal section of stage 35 embryos. The inset indicates the transcripts of *pax7* in spinal cord concentrated on the dorsal side. (H) Transverse section through the midbrain of a stage 35 embryo. (I) *Pax7* expression in the pituitary anlage is marked by an asterisk. (J,L) Transverse section through the trunk of a stage 35 embryo. (K) Parasagittal section of stage 35 embryo showing *pax7* transcripts in posterior pronephric anlage. (M) Horizontal section of stage 35 embryo head. (N) Parasagittal section of stage 35 embryo. The black arrows in H,M,N indicate the mesenchyme cells with *pax7* expression anterior to the eye. The white arrow in N indicates that *pax7* transcripts locate in the edges of myotomes. (O) Parasagittal view of the tail of stage 35 embryo. Abbreviations: e, eye; mb, midbrain; n, notochord; pa, pituitary anlage; pr, pronephros; sc, spinal cord; so, somite.

The segmented expression pattern of *pax7* is obvious in anterior dorsal lateral somites starting from stage 19 (inset in Fig. 1C). A series of faint chevrons of *pax7* expression appears in the trunk region of early tailbud stage embryo (Fig. 1D), and intensify as embryo develops (Fig. 1D-F). Parasagittal section shows that *pax7* is expressed in scattered cells at the anterior and posterior edges of individual somites (Fig. 1N) and a slight random scatter of cells in the undifferentiated presomitic mesoderm of the tail bud (Fig. 1O).

At later tadpole stages, in situ probes are unable to penetrate the tadpole skin. Therefore, we used anti-Pax7 monoclonal antibody to detect expression of Pax7 protein on paraffin sections. Consistent with our in situ results, the immunohistochemistry study shows that high levels of Pax7 expression are present in forebrain (data not shown), midbrain (Fig. 2A), hindbrain (Fig. 2B) and dorsal spinal cord (Fig. 2C). Moreover, Pax7 is expressed in the eye muscle and pituitary gland (Fig. 2A,D). The cells with Pax7 positive signals in the tadpole trunk and tail muscle are flat, peripheral and squeezed beneath the basement membrane, as revealed by laminin antibody staining (Fig. 2E). On the basis of their position, these cells are mostly likely to be muscle satellite cells.

In summary, the in situ hybridization and immunohistochemistry studies in *Xenopus laevis* demonstrate that *Xenopus pax7*, like its homologues in other species, is strongly expressed in the central nervous system and muscle. This expression pattern continues to adult stage, as detected by RT-PCR (data not shown). Apart from that, *Xenopus Pax7* is also expressed in pituitary gland (Fig. 1I and Fig. 2A) and adult testis (data not shown).

Pax7 is a reliable marker of muscle satellite cell in the tadpole tail

The expression study of Pax7 suggested that the cells squeezed between myofibres with positive Pax7 immunostaining signals may be *Xenopus* muscle satellite cells. To investigate this, we performed

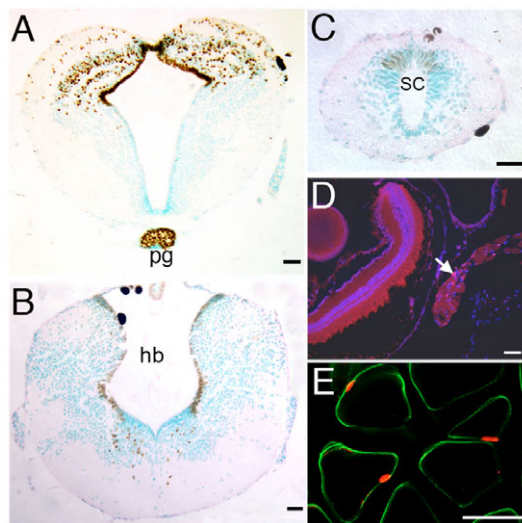


Fig. 2. Pax7 antibody detection in stage 46 tadpole.

Immunostaining with anti-Pax7 monoclonal antibody was carried out on transverse sections of stage 46 tadpoles. (A-C) Detection of Pax7 with DAB staining (brown). The tissues were counterstained with 0.5% Methyl Green solution. (A) Midbrain; (B) hindbrain; (C) spinal cord. (D) Immunostaining of Pax7 (red) and DAPI (blue) on cross-section of tadpole head. The arrow in D indicates expression of Pax7 in eye muscle. (E) Co-immunostaining of Pax7 (red) and laminin (green) on cross-section of tadpole tail muscle. Abbreviations: hb, hindbrain; mb, midbrain; pg, pituitary gland; sc, spinal cord. Scale bars: 20 μ m.

immunoelectron microscopy (IEM). Muscle satellite cells are located in dentations between the basement membrane and plasma membrane of myofibres, while the myonucleus lies within the plasma membrane of myofibres (Mauro, 1961). These morphological criteria enable us to distinguish between the nuclei of satellite cells and the myonuclei by transmission electron microscopy.

Fig. 3A,B show muscle satellite cells that are squeezed between the basal lamina (indicated by arrows in Fig. 3C,D) and the plasma membrane. The positive Pax7 antibody signals visualized by black electron dense dots concentrate in the nuclei of satellite cells. By contrast, no Pax7 antibody activity is detected in the myonuclei (Fig. 3E). Statistically, among 25 muscle satellite cells from five individual tails, 22 cells were found to be positive for Pax7 (88%, $n=25$); by contrast, all the myonuclei identified are negative for Pax7 (0%, $n=41$; Table 1). As negative control, sections stained without Pax7 antibody do not show any electron dense granules in the nucleus (data not shown). Thus, we are able to take Pax7 as a reliable muscle satellite cell marker in the tail of *Xenopus* tadpole.

Occasionally the Pax7 antibody-positive signals are also found in some other cell types in tadpole tail, outside of the muscle fibres. These cells are identified based on their characteristic structures as described in the Boston University ultrastructure website

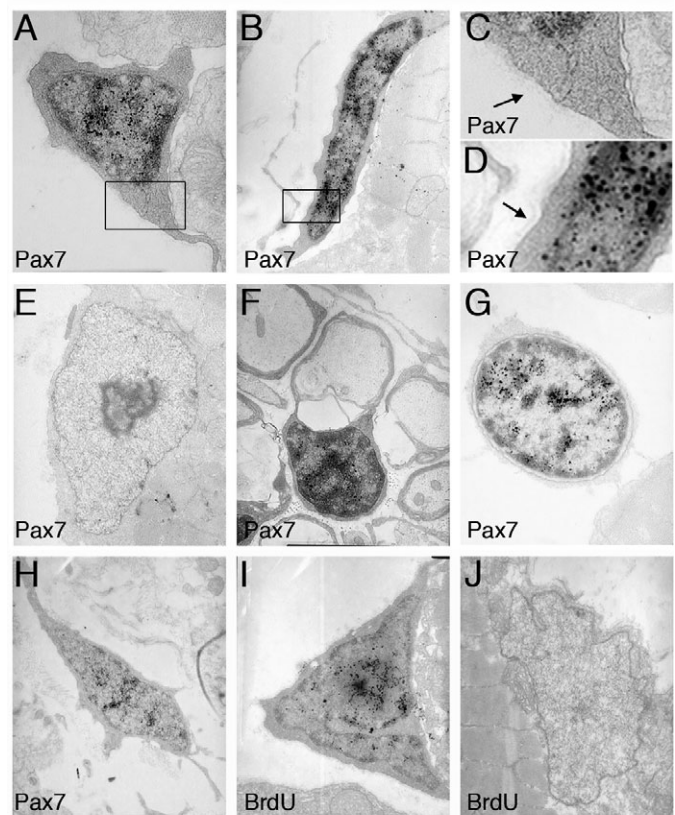


Fig. 3. Immuno-electron microscopy study of Pax7 and BrdU labelling in tadpole tail.

(A,B) Satellite cell with Pax7 antibody labelling in the nucleus. (C,D) High-power views of black box regions of A and B, respectively. The basement membrane is indicated by the arrows in C,D. (E) A myonucleus negative for Pax7 signal. (F) A Schwann cell with Pax7 antibody labelling in the nucleus. (G) A lymphocyte located between myofibres is positive for Pax7. (H) A fibroblast in the muscle connective tissues has a faint positive signal. (I) A satellite cell with BrdU labelling in the nucleus. (J) A myonucleus negative for BrdU.

Table 1. Immunoelectron microscopy study with Pax7 and BrdU labelling

	Pax7			BrdU		
	+	-	Number	+	-	Number
Satellite cell	22 (88%)	3 (12%)	25	12 (60%)	8 (40%)	20
Myonucleus	0	41 (100%)	41	1 (3.3%)	30 (96.7%)	31

(http://www.bu.edu/histology/m/t_electr.htm). The Pax7 antibody label is present in the nucleus of Schwann cells whose cell membrane forms myelin coils around the axon (Fig. 3F). A lymphocyte that is characterized by its nucleus filling virtually the entire volume of the cell is also found to be positive (Fig. 3G). Moreover, a faint Pax7-positive signal is located in the nucleus of a fibroblast surrounded with collagen fibrils (Fig. 3H). This shows that not every Pax7-positive cell in the tail is necessarily a satellite cell.

Muscle satellite cells are proliferating in the growing tail

Previously, we observed many BrdU-labelled cells in the muscle of the growing tadpoles (Gargioli and Slack, 2004). To find whether these are, in fact, satellite cells, we injected BrdU into stage 49 tadpoles and fixed the tadpole tails 1 day after injection. They were processed for immuno-electron microscopy, using antibody to BrdU. We found that 60% of satellite cell nuclei are labelled with anti-BrdU (Fig. 3I, Table 1). By contrast, almost all the myonuclei examined from four tails are negative for BrdU (Fig. 3J, Table 1). Only one myonucleus was detected with a faint BrdU antibody signal. This is perhaps due to DNA repair synthesis, or to recent incorporation of a satellite cell in the fibre. As satellite cells are multiplying and myonuclei are not, it seems highly likely that the satellite cells are the source of the new fibres, or contribute to fibre expansion during growth, as they do in mammals (Moss and Leblond, 1971).

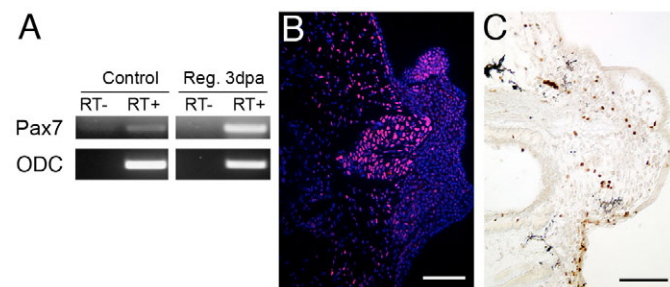


Fig. 4. Pax7 is upregulated in regenerating tadpole tails. (A) RT-PCR shows that *pax7* messenger RNA is more abundant in regenerating tails at 3 dpa, compared with the tails without amputation. (B) PCNA antibody staining (red) on parasagittal section of regenerating tail. DAPI (blue) shows the nuclei. The dense region in the centre is the notochord tip, with the blastema above and below. (C) Pax7 antibody-labelled cells (brown) on parasagittal sections of regenerating tail. Dorsal side upwards and anterior leftwards. Scale bars: 100 μ m.

Pax7 is upregulated during tail regeneration

Tails of *Xenopus* tadpole will regenerate fully after amputation (Slack et al., 2004). To test whether Pax7 plays a role in this process, we performed RT-PCR assays with regenerating tails 3 days post amputation. As shown in Fig. 4A, the *pax7* mRNA level is increased in the regenerating tails, compared with that in tails without amputation. We consider that this is due to an increase in number of Pax7-positive cells. It is not possible to make a precise quantitative comparison of cell numbers because the structure of mature tail muscle and regeneration bud are so different. However, at this stage, there is a considerable amount of cell proliferation in the regeneration bud, indicated by PCNA antibody staining (Fig. 4B), and many Pax7-positive cells are found free of the muscle lying close to the amputation level in the blastema (Fig. 4C), which is the undifferentiated region of the regeneration bud (Gargioli and Slack, 2004).

Pax7EnR is a dominant negative form of Pax7

To further investigate the function of Pax7 in muscle satellite cells during *Xenopus* tail regeneration, we generated a domain-swapped construct *pax7EnR*, in which the C-terminal region of *Xenopus* Pax7 was replaced with the transcriptional repression domain of *Drosophila* Engrailed (Han and Manley, 1993).

This method has been used many times to generate transcription factor domain swaps, but we felt it important to confirm that it really had the predicted biological activity: namely that it can inhibit normal Pax7 function. To do this, we overexpressed Pax7EnR in the brain region, which is rich in endogenous expression of Pax7. We injected 200 pg *pax7EnR*, together with 80 pg *gfp* mRNA, into the left side of the dorsal animal hemisphere of four-cell stage embryos. The injected neurulae show defects in the anterior neural fold on the left (Fig. 5A) and later on in the developing left eye (Fig. 5C and Table 2). These defects become obvious at advanced stages. The left eye is absent or smaller, while the right eye has fully developed (Fig. 5C,D,F). The GFP fluorescence on the injected side indicates that it still has a small lens underneath the epidermis (inset in Fig. 5C). To test the specificity of Pax7EnR, we co-injected the *pax7EnR* RNA together with 500 pg wild-type *pax7* RNA. As shown in Fig. 5B,E and Table 2, the *pax7* RNA is able to rescue these eyes back to approximately normal size.

The above results suggested the involvement of Pax7 in eye development in *Xenopus laevis*. As *pax7EnR* inhibits eye development, it is possible that *pax7* itself can promote eye development on overexpression. Indeed this is the case. When 500

Table 2. Summary of eye development in *pax7/pax7EnR* injected embryos

Constructs	Two normal eyes and one extra eye	Two normal eyes	One small eye and one normal eye	Single eye
<i>pax7EnR</i>	0	43 (48.8%)	32 (36.4%)	13 (14.8%)
<i>pax7EnR+pax7</i>	0	37 (94.9%)	2 (5.1%)	0
<i>pax7</i>	15 (10.0%)	135 (90.0%)	0	0

pax7EnR (200 pg) or 500 pg *pax7* capped RNA, or both, were injected into one of the dorsal animal hemispheres of four-cell stage embryos. Eye development was measured at stage 46.

pg *pax7* and 80 pg *gfp* mRNA were co-injected into one side of the dorsal animal hemisphere at the four-cell stage, some tadpoles developed an ectopic eye at the injected site (Fig. 5G-I, Table 2). Although only a small proportion of the injected tadpoles developed an ectopic eye, when found it is very well formed, containing a retinal pigmented epithelial layer, outer nuclear layer, inner nuclear layer, ganglion cell layer and lens in a spatial arrangement identical to the endogenous eyes. Detailed examination of these tadpoles shows that the ectopic eye is often accompanied by a tube protruding from ventral midbrain (Fig. 5J). No ectopic eyes were seen in tadpoles resulting from embryos injected into the same region with *gfp* mRNA alone.

We are not claiming that Pax7 has a normal function in *Xenopus* eye development, but the phenomena described here provide us with a useful bioassay. The experiments show that Pax7 promotes eye

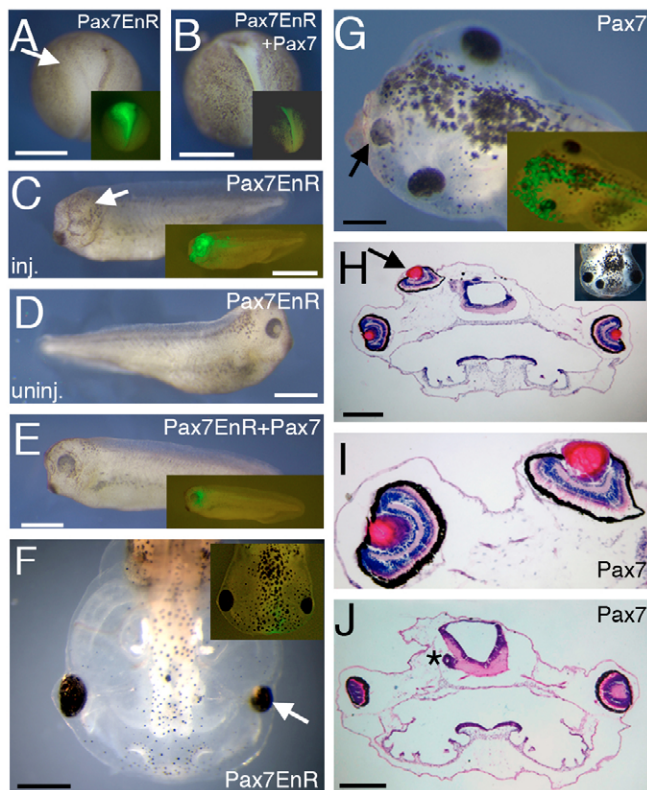


Fig. 5. Pax7EnR functions as a dominant-negative form of Pax7. (A, C, D, F) Embryos injected with 200 pg *pax7EnR* mRNA and 80 pg *GFP* into left side of dorsal animal hemisphere at four cell stage. (A) A stage16 embryo; the arrow indicates the anterior neural fold defect on left-hand side. (C) Left side of *pax7EnR* injected embryo, the arrow indicates the developing eye. The fluorescence in the inset shows a small lens underneath the epidermis. (D) Eye development on the uninjected side. (F) A tadpole with a smaller left eye (arrows). (B, E) Co-injection of 500 pg *pax7* mRNA, 200 pg *pax7EnR* mRNA and 80 pg *GFP* is able to rescue the defective eyes to normal size. (G) Injection of 500 pg *pax7* and 80 pg *gfp* mRNA into one side of the dorsal animal hemisphere results in an ectopic eye in the forebrain of stage 43 tadpoles. The GFP fluorescence in the insets indicates the injected region. (H-J) Transverse sections through ectopic eye of injected tadpole (shown in inset) were stained with Hematoxylin and Eosin. The arrows in G, H indicate the extra eyes. (I) A magnified view of the ectopic eye and one normal eye. The asterisk in J highlights the tube protruding from the ventral midbrain. Scale bars: 300 μ m.

development, Pax7EnR represses it and sufficient Pax7 can restore eye development in the presence of Pax7EnR. This proves that Pax7EnR is able to inhibit the function of Pax7 and we can therefore use Pax7EnR as a dominant-negative form of Pax7 to investigate the function of Pax7 during muscle regeneration.

The number of muscle satellite cells is decreased in heat shocked *pax7EnR* transgenic tails

As the RNA experiments showed that overexpression of Pax7EnR disturbs the early embryonic development of *Xenopus laevis*, we generated transgenic tadpoles in which the *pax7EnR* gene is driven by a heat-shock promoter in response to a 34°C warm pulse (Beck et al., 2003). This means that the gene is inactive through development and activated only when the temperature is raised. We performed RT-PCR analysis on four groups of tadpole tails. They are: (1) wild-type

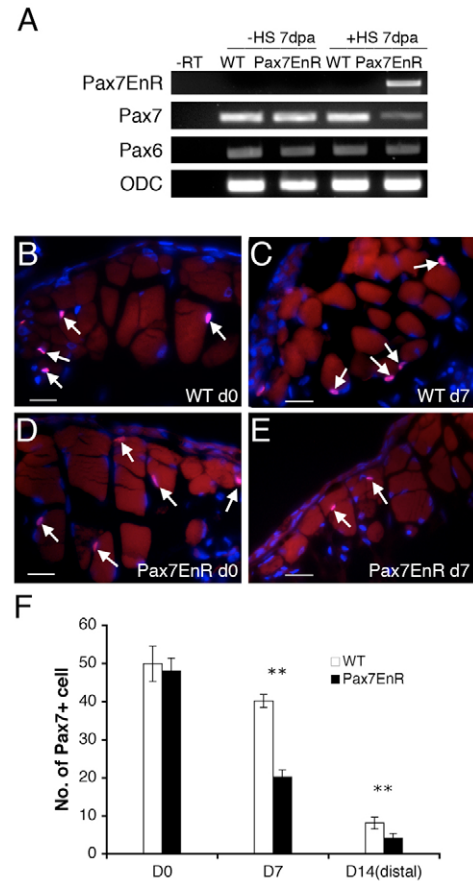


Fig. 6. The number of muscle satellite cells is reduced in the heat shocked *pax7EnR* transgenic tails. (A) RT-PCR detection of *pax7*, *pax6* and *pax7EnR* in wild-type and *pax7EnR* transgenic tadpoles with or without heat shock treatment. (B-E) The expression of Pax7 (red) in transverse sections of the tails. (B) Wild-type tail. (C) Wild-type regenerating tail with daily heat shock for 7 days after amputation. (D) *pax7EnR* transgenic tail. (E) *pax7EnR* transgenic regenerating tail with daily heat shock for seven days after amputation. (F) The histogram shows the number of satellite cells quantified by Pax7 antibody staining. Ten tails of similar size were examined in each case. ** $P < 0.05$. The d7 bars refer to 7-day regenerates. The d14 bars refer to 14-day regenerates amputated at a more distal level to provoke a second regeneration. Because of the more distal position, the absolute cell numbers per section are lower, but the wild type still has about twice the number of satellite cells compared with the heat-shocked *pax7EnR*. Scale bars: 20 μ m.

tails regenerated for 7 days without heat shock; (2) *pax7EnR* transgenic tails regenerated for 7 days without heat shock; (3) wild-type tails regenerated for 7 days with one heat shock each day after amputation; and (4) *pax7EnR* transgenic tails regenerated for 7 days with one heat shock each day after amputation. As shown in Fig. 6A, *pax7EnR* is induced only in the case of *pax7EnR* transgenic tails with heat shock, and no leaking expression of *pax7EnR* is detected in tails without heat shock. These results also show that the endogenous *pax7* mRNA is reduced in the regenerating tails with Pax7EnR expression. By contrast, there is no effect on *pax6* mRNA, which is also present in the regenerating tail (Fig. 6A).

The reduction of *pax7* level might arise from repression of transcription or from a reduction in the number of cells expressing *pax7*. To investigate these possibilities we compared the number of muscle satellite cells in wild-type and *pax7EnR* regenerates. Both wild-type and *pax7EnR* transgenic tadpoles were given the first heat shock three hours before tail amputation. Then the distal 50% of the tail was cut off and sectioned to generate the samples: wild type d0 and Pax7EnR d0. During tail regeneration, a heat shock was administered once every day. Seven days later, the regenerating tails were fixed as the samples wild type d7 and Pax7EnR d7. We counted the number of muscle satellite cells in the 50 μ m tail region that is nearest to the amputation surface. Based on Pax7 antibody staining of ten tails of each group, we found the number of satellite cells in wild type d0 and Pax7EnR d0 is similar (Fig. 6B,D,F). After 7 days regeneration, the number of satellite cells falls a little in the wild-type regenerates but falls substantially in the *pax7EnR* regenerates (Fig. 6C,E,F). After 14 days regeneration, the number of satellite cells in the *pax7EnR* tadpoles was still about half the number in wild type (Fig. 6F). The 14-day sections are from a more distal level of the regenerate, corresponding to the level of second amputation (see

below), and so the absolute cell numbers per section are much reduced owing to the smaller area. For all the specimens, the level of Pax7 in the satellite cells appears approximately similar, indicating that the reduction of *pax7* mRNA level by Pax7EnR arises from a reduction in the number of satellite cells.

Pax7EnR causes cell death during muscle regeneration

The reduction of the number of muscle satellite cells in *pax7EnR* transgenic tails might arise from a reduction in the normal proliferation or from promotion of cell death of satellite cells during muscle regeneration. We examined cell proliferation by PCNA antibody staining in 3 day regenerating tails of wild-type and *Pax7EnR* transgenic tadpoles and this showed no obvious difference (data not shown).

Then, we performed TUNEL staining to test for apoptosis in the regenerating tails. In the case of *pax7EnR* transgenic tails, the same location that muscle satellite cells are found freed from the myofibres (Fig. 7A-C). In the wild-type tails, the number of apoptotic cells is smaller than that in the *pax7EnR* transgenic tails (Fig. 7E). Moreover, in many clusters of cells, possibly indicating small clones, those with low level of Pax7 expression are often entering apoptosis (red arrows in Fig. 7D), although those with high level of Pax7 expression are not. Given that the heat shock promoter is expected to have a similar activity in all cells, it may be that the cells with lower content of *pax7* are more vulnerable to the effect of the *pax7EnR*. Quantification of cell death shows that cell death in mesenchyme and blastema of *pax7EnR* transgenic tails is more severe than that in wild-type tails, whereas cell death in the regenerating spinal cord and notochord is unaffected (Fig. 7E).

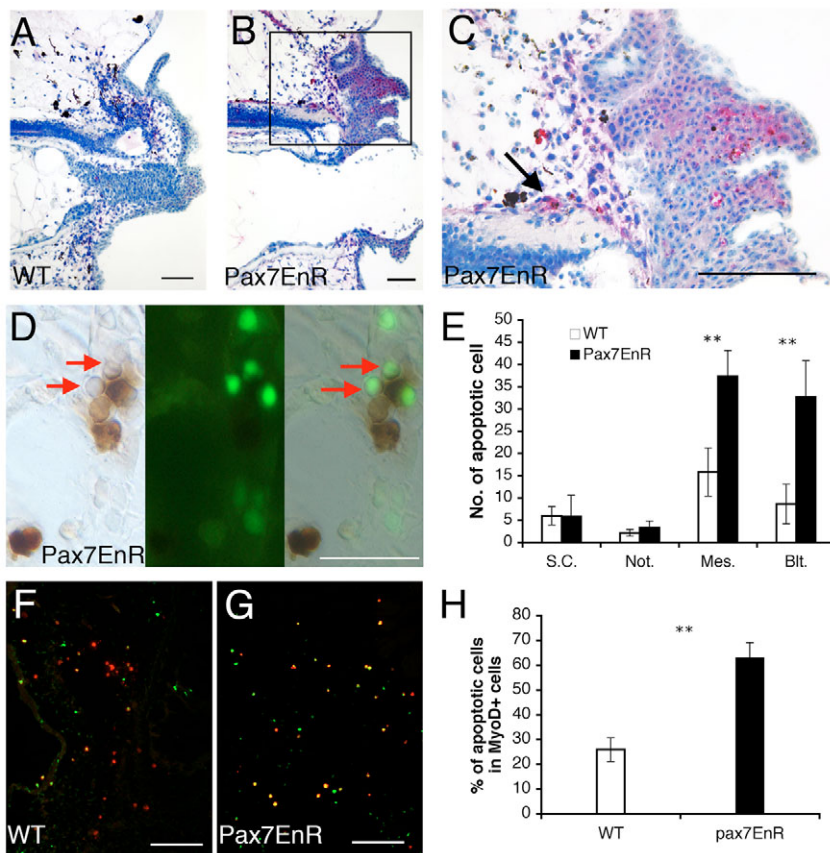


Fig. 7. Pax7EnR promotes satellite cell apoptosis during tail regeneration.

(A-C) TUNEL assays were performed on parasagittal sections of regenerated tail at 3 dpa; the colour was developed with a Fast Red tablet and counterstained with Mayor's Hematoxylin. (A) Wild-type regenerated tail. (B) Heat-shocked *pax7EnR* transgenic regenerated tail. (C) Higher power view of B. TUNEL signals in the blastema region are arrowed. (A-C) Dorsal side upwards, anterior towards left. (D) Detection of Pax7 with DAB staining (left panel) and apoptosis with fluorescein labelling (middle panel), in a cluster of cells in *pax7EnR* transgenic tail. The right panel is the merged view. Red arrows: two TUNEL-positive/Pax7 low expression cells. (E) Quantification of the number of apoptotic cells in the two groups of tails. (F,G) Detection of MyoD (red) and cell death (green) on parasagittal sections of regenerated tails at 3 dpa. (F) Blastema region of wild-type tail. (G) Blastema region of heat-shocked *pax7EnR* tails. (H) Quantification of the percentage of apoptotic cells among the MyoD-positive cells in the two groups of tails. Ten tails of similar size were examined in each group. ** $P < 0.01$. Abbreviations: S.C., spinal cord; Not., notochord; Mes., mesenchyme; Blit., blastema. Scale bars: 100 μ m.

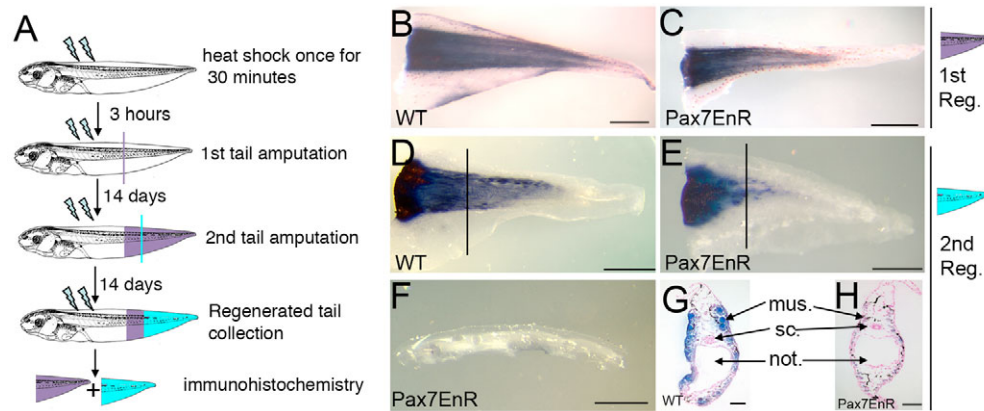


Fig. 8. 12/101 staining of regenerating tails in wild-type and *pax7EnR* transgenic tadpoles. (A) The flowchart in the experiment of repeated tail amputation. The first heat shock is given 3 hours before the first amputation and heat shocks are given daily thereafter. The distal 50% tail was cut in the first tail amputation. The second tail amputation was performed at 14 dpa at the site of distal 75% of the first regenerated tail. The purple and blue tails indicate the primary and secondary regenerated tail, respectively. (B-F) 12/101 antibody staining of the regenerated tails. (B) Wild-type tails 14 days post first amputation. (C) *pax7EnR* transgenic tails 14 days post first amputation. (D) Wild-type regenerated tails, 14 days after second amputation. (E,F) *pax7EnR* regenerated tails 14 days after second amputation. (G,H) Transverse section of second regenerated tail in wild type (G) and *pax7EnR* transgenic tadpoles (H). Section level is indicated by the black lines in D,E. Abbreviations: sc, spinal cord; not., notochord; mus, muscle. Scale bars: 500 μm in B-F; 50 μm in G,H.

To further investigate apoptosis of muscle satellite cells during regeneration, we used the MyoD antibody (Hopwood et al., 1992) to label the activated satellite cells (Zammit et al., 2004) and then performed a TUNEL assay. The cell quantification result demonstrates that over 60% of MyoD-labelled cells in the mesenchyme and blastema region of *pax7EnR* transgenic tails are undergoing apoptosis, whereas only 25% of MyoD-positive cells undergo apoptosis in wild-type tails. This result confirms a protective role of Pax7 in cell survival, something that has also been noticed in mammalian studies (Kuang et al., 2006; Relaix et al., 2006). In other words, Pax7EnR reduces the number of satellite cells not by reducing their proliferation rate but by increasing their rate of cell death.

Muscle regeneration is inhibited in *pax7EnR* transgenics

The above results show that the number of satellite cells in regenerating tails is sharply decreased when *pax7EnR* is activated by heat shock. So we predict that less muscle would form in the regenerating *pax7EnR* transgenic tails compared with wild type, if muscle satellite cells are the sole source of muscle regeneration. However, after 14 days heat-shock treatment, when muscle in wild-type tail has terminally differentiated, we did not find a significant reduction of muscle in the transgenic *pax7EnR* tails. As shown in Fig. 8B,C, the staining strength of 12/101, a marker of muscle differentiation, is similar in *pax7EnR* and in wild-type tails.

However, we know that the first regenerate is depleted in satellite cells and this raises the question of whether it can regenerate yet more muscle following a second amputation. To investigate this, we followed the procedure as depicted in Fig. 8A. The Pax7EnR expression is induced with a daily heat shock throughout the

regeneration period. The first regenerate is allowed to grow for 14 days and then the distal 75% of the primary regenerated tail is re-amputated and allowed to regenerate for another 14 days. As shown in Fig. 6F, the number of satellite cells in heated *pax7EnR* transgenics is about half that in wild types at this amputation level. After the second regeneration, we performed 12/101 immunostaining on both regenerates. As shown in Fig. 8B,D,G, the muscle in both first and second regenerates of wild-type tails was fully formed. By contrast, for the case of *pax7EnR* heat shocked tadpoles, 61% of the second tail regenerates showed substantially reduced differentiated muscle, and another 11% had no muscle at all (Fig. 8E,F, Table 3). In these individuals the spinal cord and the notochord do regenerate fully in the second regenerate, so even though Pax7 is expressed in some spinal cord cells it is presumably not necessary for regeneration (Fig. 8H). This experiment clearly shows that the regeneration of muscle depends on the presence of a population of satellite cells in the amputated tail.

DISCUSSION

Expression of Pax7

Our *in situ* hybridization and immunohistochemistry studies suggest that *pax7* expression is highly conserved in vertebrates. As in mouse and chick, *pax7* transcripts in *Xenopus* are mainly found in the central nervous system, the embryonic muscle and in muscle satellite cells. *pax7* expression in embryonic brain and spinal cord shows high regional specificity, as indicated by its dorsal expression in midbrain and the whole spinal cord, with ventral expression in a subpopulation of neural cells in the hindbrain (Figs 1, 2). This *pax7* expression pattern is similar to that in mouse and chick (Jostes et al., 1990; Kawakami et al., 1997). During embryonic myogenesis, the chevron pattern observed in *Xenopus* somites is very similar to the

Table 3. Muscle regeneration in wild-type and *pax7EnR* transgenic tadpole tails

Transgene	HS first amputation				HS second amputation			
	None	Partial	Complete	<i>n</i>	None	Partial	Complete	<i>n</i>
Wild-type control	0	0	40 (100%)	40	0	0	32 (100%)	32
<i>pax7EnR</i>	0	0	35 (100%)	35	3 (11%)	17 (61%)	8 (28%)	28

Pax7 expression pattern in the E12.5 mouse myotome (Horst et al., 2006). Expression of *pax7* is also observed in a subset of muscle cells, with the position and appearance of satellite cells (Fig. 2). This similar expression pattern suggests a conserved involvement of *pax7* in embryonic myogenesis and specification of muscle progenitor cells (Halevy et al., 2004; Seale et al., 2004; Gros et al., 2005; Kassam-Duchossoy et al., 2005; Relaix et al., 2005).

However, there exist minor differences of *pax7* expression profile between species. *pax7* expression is found in the melanocyte lineage in chick and quail, but not in the melanocyte lineage in *Xenopus* tadpoles, mouse and rat (Lacosta et al., 2005). Expression of *pax7* in head mesenchyme is also different in *Xenopus* and mouse. As shown in Fig. 1H,M,N, *pax7* transcripts appear earlier and stronger than that in the segmented somites, while in mouse, *pax7* expression in the head mesenchyme is not detectable until E11.5 (Horst et al., 2006).

The presence of *pax7* transcripts in the pronephros of the *Xenopus* embryo is interesting and its function during organogenesis is currently under investigation. Our preliminary result suggests that *pax7* also plays an important role in the growing pronephros, probably synergizing with Pax2 and Pax8 by acting as an anti-apoptotic factor (Y.C., G.L. and J.M.W.S., unpublished) (Relaix et al., 2006).

Pax7 in eye development

Our testing of the function of *pax7* and *pax7EnR* constructs by injecting them into the dorsal side of four-cell stage embryos resulted in a very surprising phenotype: the induction of a well-formed extra eye. This phenotype is reproducible, despite the low frequency of occurrence (10% of cases). In an elegant manner, this overexpression phenotype is the 'opposite' of the Pax7EnR phenotype, which involves reduction of the normal eye. The eye-reduction phenotypes of *pax7EnR* can be rescued by co-injection of *pax7*. An overexpression phenotype does not, of course, prove that the gene in question is involved in the normal development of the affected structure. In this case, it is probably not directly involved as Pax7 is not normally expressed in the eye itself. However, it is expressed in the region immediately anterior to the eye and so the overexpression effects may indicate an indirect function for Pax7 in eye development involving signals from the surrounding tissues.

Consistent with this, *pax7* is expressed in chick optic tectum and mouse superior colliculus, one of the major visual targets in brain (Nomura et al., 1998; Ziman et al., 2001b; Thomas et al., 2004; Thompson et al., 2004). When misexpressed, Pax7 can induce ectopic formation of superior collicular tissue, with characteristic laminae innervated by retinal ganglion cell axons (Matsunaga et al., 2001; Thompson et al., 2004). Interestingly, among the tadpoles with an extra eye, we very often observed formation of an extra tube-like structure protruding from the midbrain (asterisks in Fig. 5J). Detection of a series of transcription factors related to eye field specification show that some of the transcription factors, such as Rx1 and Tll, are downregulated by *pax7EnR* injection (data not shown). Thus, these findings do support a role of Pax7 in the development and maturation of the vertebrate visual system, even if it is indirect. It is also possible that the overexpression experiments are interfering in some way with *pax6*, well known as a master controlling gene in eye development (Gehring and Ikeo, 1999). However, Fig. 6A does not indicate any effect on *pax6*, at least at the level of mRNA content.

Pax7 as a satellite cell marker

In this report, we show that Pax7 is a reliable satellite cell marker by combining nuclear Pax7 expression with morphological observations of satellite cells by electron microscopy. We need a

good molecular marker, because it is impossible reliably to identify a satellite cell under light microscope by morphology alone. As shown in Fig. 3 and our statistical analysis, the immuno-electron microscope result proves that Pax7 is a very good satellite cell marker. The observation that 88% of morphologically identified satellite cells express Pax7 would allow us to pick up most of satellite cells in a pool of cell population. The minority of negative cells are presumably those that have commenced differentiation to myoblasts. Despite the occasional expression of Pax7 in other cell types, expression of Pax7 in myonuclei is never found, providing a very clear discrimination between the satellite cells and myofibres themselves. The presence of Pax7 in some Schwann cells may possibly be associated with their ability to re-enter the cell cycle for peripheral nerve regeneration (Hall, 2005).

Several other molecules, including neural cell adhesion molecule (NCAM), Met and M-cadherin, have been used to identify satellite cells in various experimental approaches (for a review, see Holterman and Rudnicki, 2005), so we also checked the expression of these candidates in *Xenopus*. In our hands, the efficiency of negative markers to recognize satellite cells in *Xenopus* tadpoles is not as good as for Pax7. We observed significantly more Pax7-positive cells in tadpole muscle tissues than cells positive for other markers (data not shown) and so consider Pax7 as the most reliable satellite cell marker in *Xenopus*.

Cell origin of muscle regeneration in *Xenopus* tadpoles

Our results support our previous conjecture that satellite cells residing in the tail muscle fibres are the origin of muscle regeneration in *Xenopus* tadpoles (Gargioli and Slack, 2004). First, additional expression of *pax7* in the regenerating tail suggests that satellite cells are activated to divide after tail amputation. In regenerating tails 3 days post amputation, a large number of Pax7-positive cells appears in the region where muscle fibres are undergoing degeneration, and many Pax7-positive cells are visible in the growing blastema (Fig. 4). Second, our experiments show that inhibition of Pax7 action by Pax7EnR causes apoptosis of muscle satellite cells, and reduces the number of satellite cells in regenerating tails. The tails that are depleted of satellite cells do still regenerate, but most regenerates contain little or no muscle (Fig. 8; Table 3). Thus, our result demonstrates that muscle regeneration in *Xenopus* tails is similar to muscle repair in mammals, where it has been generally accepted that satellite cells are adult muscle precursor cells and contribute to repair of damaged muscle (Wagers and Conboy, 2005). The actual requirement for Pax7 function must be in the survival of the proliferating satellite cells rather than in their differentiation into muscle, as the ability to form a first regenerate is not significantly impaired. This is consistent with the observed loss of Pax7 expression on differentiation (Seale and Rudnicki, 2000).

Recent studies have demonstrated that Pax7 has an important role in cell survival of adult muscle satellite cells (Kuang et al., 2006; Relaix et al., 2006). Using activated caspase 3 as a marker, Relaix et al. showed that apoptosis occurs in activated satellite cells in the skeletal muscle of the *pax7* mutant (Relaix et al., 2006). Consistent with this, our detection of cell death with TUNEL assay suggest that cells with low level of Pax7 tend to undergo apoptosis, while those with high level of Pax7 expression can be protected from dying. In the regenerating tails of *pax7EnR* tadpoles, the number of cells undergoing apoptosis is increased (Fig. 7) and this ultimately results in the failure of regeneration of muscles in *pax7EnR* transgenic tails.

It was found that Pax3, which is expressed both in quiescent and activated muscle satellite cells in mammals, has partially redundant function with Pax7 in satellite cells (Relaix et al., 2005; Relaix et al., 2006). As we do not obtain 100% suppression of muscle regeneration with *pax7EnR*, it is possible that there is a redundant component present such as Pax3, but it is also possible that we do not obtain 100% inhibition of pax7 function.

Our experiments do not support the view that myofibres regenerate from resident or circulating stem cells of the side population (SP) type (Chargé and Rudnicki, 2004). As discussed above, these stem cells should be available to reconstitute the muscle fibres in *pax7EnR* tadpoles but do not do so. Our results also differ from the previous findings on limb regeneration in newts and axolotl, in which it has been well documented that de-differentiation and re-differentiation of multinucleate muscle fibres occurs (Lo et al., 1993; Kumar et al., 2000; Echeverri et al., 2001; Echeverri and Tanaka, 2002). We see no particular reason to doubt the results from the urodele species but consider that the mode of *Xenopus* tail muscle regeneration to be much closer to the regeneration of damaged muscle in mammals. Interestingly, a recent paper on newt regeneration has also highlighted a role for satellite cells (Morrison et al., 2006).

Together, our experiments support the idea that Pax7 is required for the survival of the proliferating satellite cells in muscle and hence the maintenance of the satellite cell pool during regeneration (Kuang et al., 2006; Relaix et al., 2006). This satellite cell pool is the origin of the regenerated muscle in the *Xenopus* tadpole tail.

We thank Dr Ian Jones and Mrs Ursula Potter for technical advice on immunoelectron microscopy. We also thank Drs John Gurdon and Henrietta Standley for giving us the monoclonal antibody specific for *Xenopus laevis* MyoD. This work was supported by a Wellcome Trust Programme grant to J.M.W.S.

References

- Amaya, E. and Kroll, K. L. (1999). A method for generating transgenic frog embryos. *Methods Mol. Biol.* **97**, 393-414.
- Beck, C. W., Christen, B. and Slack, J. M. W. (2003). Molecular pathways needed for regeneration of spinal cord and muscle in a vertebrate. *Dev. Cell* **5**, 429-439.
- Chargé, S. B. and Rudnicki, M. A. (2004). Cellular and molecular regulation of muscle regeneration. *Physiol. Rev.* **84**, 209-238.
- Collins, C. A., Olsen, I., Zammit, P. S., Heslop, L., Petrie, A., Partridge, T. A. and Morgan, J. E. (2005). Stem cell function, self-renewal, and behavioral heterogeneity of cells from the adult muscle satellite cell niche. *Cell* **122**, 289-301.
- Cooper, R. N., Tajbakhsh, S., Mouly, V., Cossu, G., Buckingham, M. and Butler-Browne, G. S. (1999). In vivo satellite cell activation via Myf5 and MyoD in regenerating mouse skeletal muscle. *J. Cell Sci.* **112**, 2895-2901.
- Cornelison, D. D. and Wold, B. J. (1997). Single-cell analysis of regulatory gene expression in quiescent and activated mouse skeletal muscle satellite cells. *Dev. Biol.* **191**, 270-283.
- Echeverri, K. and Tanaka, E. M. (2002). Ectoderm to mesoderm lineage switching during axolotl tail regeneration. *Science* **298**, 1993-1996.
- Echeverri, K., Clarke, J. D. and Tanaka, E. M. (2001). In vivo imaging indicates muscle fiber dedifferentiation is a major contributor to the regenerating tail blastema. *Dev. Biol.* **236**, 151-164.
- Gargioli, C. and Slack, J. M. W. (2004). Cell lineage tracing during *Xenopus* tail regeneration. *Development* **131**, 2669-2679.
- Gehring, W. J. and Ikeo, K. (1999). Pax 6, mastering eye morphogenesis and eye evolution. *Trends Genet.* **15**, 371-377.
- Gros, J., Manceau, M., Thomae, V. and Marcelle, C. (2005). A common somitic origin for embryonic muscle progenitors and satellite cells. *Nature* **435**, 954-958.
- Gussoni, E., Soneoka, Y., Strickland, C. D., Buzney, E. A., Khan, M. K., Flint, A. F., Kunkel, L. M. and Mulligan, R. C. (1999). Dystrophin expression in the mdx mouse restored by stem cell transplantation. *Nature* **401**, 390-394.
- Halevy, O., Piastun, Y., Allouh, M. Z., Rosser, B. W., Rinkevich, Y., Reshef, R., Rozenboim, I., Wleklinski-Lee, M. and Yablonka-Reuveni, Z. (2004). Pattern of Pax7 expression during myogenesis in the posthatch chicken establishes a model for satellite cell differentiation and renewal. *Dev. Dyn.* **231**, 489-502.
- Hall, S. (2005). The response to injury in the peripheral nervous system. *J. Bone Joint Surg. Br.* **87**, 1309-1319.
- Han, K. and Manley, J. L. (1993). Functional domains of the *Drosophila* Engrailed protein. *EMBO J.* **12**, 2723-2733.
- Harland, R. M. (1991). In situ hybridization: an improved whole-mount method for *Xenopus* embryos. *Methods Cell Biol.* **36**, 685-695.
- Holtzman, C. E. and Rudnicki, M. A. (2005). Molecular regulation of satellite cell function. *Semin. Cell Dev. Biol.* **16**, 575-584.
- Hopwood, N. D., Pluck, A., Gurdon, J. B. and Dilworth, S. M. (1992). Expression of XMyoD protein in early *Xenopus laevis* embryos. *Development* **114**, 31-38.
- Horst, D., Ustanina, S., Sergi, C., Mikuz, G., Juergens, H., Braun, T. and Vorobyov, E. (2006). Comparative expression analysis of Pax3 and Pax7 during mouse myogenesis. *Int. J. Dev. Biol.* **50**, 47-54.
- Jackson, K. A., Mi, T. and Goodell, M. A. (1999). Hematopoietic potential of stem cells isolated from murine skeletal muscle. *Proc. Natl. Acad. Sci. USA* **96**, 14482-14486.
- Jostes, B., Walther, C. and Gruss, P. (1990). The murine paired box gene, Pax7, is expressed specifically during the development of the nervous and muscular system. *Mech. Dev.* **33**, 27-37.
- Kassar-Duchossoy, L., Giacone, E., Gayraud-Morel, B., Jory, A., Gomes, D. and Tajbakhsh, S. (2005). Pax3/Pax7 mark a novel population of primitive myogenic cells during development. *Genes Dev.* **19**, 1426-1431.
- Kawakami, A., Kimura-Kawakami, M., Nomura, T. and Fujisawa, H. (1997). Distributions of PAX6 and PAX7 proteins suggest their involvement in both early and late phases of chick brain development. *Mech. Dev.* **66**, 119-130.
- Kintner, C. R. and Brockes, J. P. (1984). Monoclonal antibodies identify blastemal cells derived from dedifferentiating limb regeneration. *Nature* **308**, 67-69.
- Kuang, S., Chargé, S. B., Seale, P., Huh, M. and Rudnicki, M. A. (2006). Distinct roles for Pax7 and Pax3 in adult regenerative myogenesis. *J. Cell Biol.* **172**, 103-113.
- Kumar, A., Velloso, C. P., Imokawa, Y. and Brockes, J. P. (2000). Plasticity of retrovirus-labelled myotubes in the newt limb regeneration blastema. *Dev. Biol.* **218**, 125-136.
- Lacosta, A. M., Muniesa, P., Ruberte, J., Sarasa, M. and Dominguez, L. (2005). Novel expression patterns of Pax3/Pax7 in early trunk neural crest and its melanocyte and non-melanocyte lineages in amniote embryos. *Pigment Cell Res.* **18**, 243-251.
- Lamey, T. M., Koenders, A. and Ziman, M. (2004). Pax genes in myogenesis: alternate transcripts add complexity. *Histol. Histopathol.* **19**, 1289-1300.
- Lo, D. C., Allen, F. and Brockes, J. P. (1993). Reversal of muscle differentiation during urodele limb regeneration. *Proc. Natl. Acad. Sci. USA* **90**, 7230-7234.
- Mansouri, A., Stoykova, A., Torres, M. and Gruss, P. (1996). Dysgenesis of cephalic neural crest derivatives in Pax7-/- mutant mice. *Development* **122**, 831-838.
- Mansouri, A., Goudreau, G. and Gruss, P. (1999). Pax genes and their role in organogenesis. *Cancer Res.* **59**, 1709s-1710s.
- Matsunaga, E., Araki, I. and Nakamura, H. (2001). Role of Pax3/7 in the tectum regionalization. *Development* **128**, 4069-4077.
- Mauro, A. (1961). Satellite cell of skeletal muscle fibers. *J. Biophys. Biochem. Cytol.* **9**, 493-495.
- Montarras, D., Morgan, J., Collins, C., Relaix, F., Zaffran, S., Cumano, A., Partridge, T. and Buckingham, M. (2005). Direct isolation of satellite cells for skeletal muscle regeneration. *Science* **309**, 2064-2067.
- Morrison, J. I., Loof, S., He, P. and Simon, A. (2006). Salamander limb regeneration involves the activation of a multipotent skeletal muscle satellite cell population. *J. Cell Biol.* **172**, 433-440.
- Moss, F. P. and Leblond, C. P. (1971). Satellite cells as the source of nuclei in muscles of growing rats. *Anat. Rec.* **170**, 421-435.
- Namenwirth, M. (1974). The inheritance of cell differentiation during limb regeneration in the axolotl. *Dev. Biol.* **41**, 42-56.
- Nieuwkoop, P. D. and Faber, J. (1967). *Normal Table of Xenopus laevis (Daudin)*. Amsterdam: North-Holland.
- Nomura, T., Kawakami, A. and Fujisawa, H. (1998). Correlation between tectum formation and expression of two PAX family genes, PAX7 and PAX6, in avian brains. *Dev. Growth Differ.* **40**, 485-495.
- Oustanina, S., Hause, G. and Braun, T. (2004). Pax7 directs postnatal renewal and propagation of myogenic satellite cells but not their specification. *EMBO J.* **23**, 3430-3439.
- Relaix, F., Rocancourt, D., Mansouri, A. and Buckingham, M. (2005). A Pax3/Pax7-dependent population of skeletal muscle progenitor cells. *Nature* **435**, 948-953.
- Relaix, F., Montarras, D., Zaffran, S., Gayraud-Morel, B., Rocancourt, D., Tajbakhsh, S., Mansouri, A., Cumano, A. and Buckingham, M. (2006). Pax3 and Pax7 have distinct and overlapping functions in adult muscle progenitor cells. *J. Cell Biol.* **172**, 91-102.
- Ryffel, G. U., Werdien, D., Turan, G., Gerhards, A., Goosses, S. and Senkel, S. (2003). Tagging muscle cell lineages in development and tail regeneration using Cre recombinase in transgenic *Xenopus*. *Nucleic Acids Res.* **31**, 1044-1051.

- Seale, P. and Rudnicki, M. A.** (2000). A new look at the origin, function, and "stem-cell" status of muscle satellite cells. *Dev. Biol.* **218**, 115-124.
- Seale, P., Sabourin, L. A., Girgis-Gabardo, A., Mansouri, A., Gruss, P. and Rudnicki, M. A.** (2000). Pax7 is required for the specification of myogenic satellite cells. *Cell* **102**, 777-786.
- Seale, P., Asakura, A. and Rudnicki, M. A.** (2001). The potential of muscle stem cells. *Dev. Cell* **1**, 333-342.
- Seale, P., Ishibashi, J., Scime, A. and Rudnicki, M. A.** (2004). Pax7 is necessary and sufficient for the myogenic specification of CD45+:Sca1+ stem cells from injured muscle. *PLoS Biol.* **2**, E130.
- Slack, J. M. W., Beck, C. W., Gargioli, C. and Christen, B.** (2004). Cellular and molecular mechanisms of regeneration in *Xenopus*. *Philos. Trans. R. Soc. Lond. B Biol. Sci.* **359**, 745-751.
- Thomas, M., Lasic, S., Beazley, L. and Ziman, M.** (2004). Expression profiles suggest a role for Pax7 in the establishment of tectal polarity and map refinement. *Exp. Brain Res.* **156**, 263-273.
- Thompson, J., Lovicu, F. and Ziman, M.** (2004). The role of Pax7 in determining the cytoarchitecture of the superior colliculus. *Dev. Growth Differ.* **46**, 213-218.
- Wagers, A. J. and Conboy, I. M.** (2005). Cellular and molecular signatures of muscle regeneration: current concepts and controversies in adult myogenesis. *Cell* **122**, 659-667.
- Zammit, P. S., Golding, J. P., Nagata, Y., Hudon, V., Partridge, T. A. and Beauchamp, J. R.** (2004). Muscle satellite cells adopt divergent fates: a mechanism for self-renewal? *J. Cell Biol.* **166**, 347-357.
- Ziman, M. R., Thomas, M., Jacobsen, P. and Beazley, L.** (2001a). A key role for Pax7 transcripts in determination of muscle and nerve cells. *Exp. Cell Res.* **268**, 220-229.
- Ziman, M. R., Rodger, J., Chen, P., Papadimitriou, J. M., Dunlop, S. A. and Beazley, L. D.** (2001b). Pax genes in development and maturation of the vertebrate visual system: implications for optic nerve regeneration. *Histol. Histopathol.* **16**, 239-249.